Published paper
Goodyer, C.E., Berzins, M., Jimack, P.K. and Scales, L.E. (2006) *A grid-enabled problem solving environment for parallel computational engineering design.* Advances in Engineering Software, 37 (7). pp. 439-449.

A Grid-enabled Problem Solving Environment for Parallel Computational Engineering Design

C.E. Goodyer[1], M. Berzins[1], P.K. Jimack[1] and L.E. Scales[1,2]

[1] School of Computing, The University of Leeds, Leeds, LS2 9JT

[2] Shell Global Solutions, Cheshire Innovation Park, Chester, CH1 3SH

Abstract

This paper describes the development and application of a piece of engineering software that provides a Problem Solving Environment (PSE) capable of launching, and interfacing with, computational jobs executing on remote resources on a computational Grid. In particular it is demonstrated how a complex, serial, engineering optimisation code may be efficiently parallelised, Grid-enabled and embedded within a PSE. The environment is highly flexible, allowing remote users from different sites to collaborate, and permitting computational tasks to be executed in parallel across multiple Grid resources, each of which may be a parallel architecture. A full working prototype has been built and successfully applied to a computationally demanding engineering optimisation problem. This particular problem stems from elastohydrodynamic lubrication and involves optimising the computational model for a lubricant based on the match between simulation results and experimentally observed data.

Keywords: Parallel, Computational Grid, Problem Solving Environments

1 Introduction

The use of numerical simulation as part of the engineering design process is now commonplace. A major constraint on its applicability, however, is provided by the computational resources within an organisation, or sub-unit within the organisation. The

use of computational Grids, either across a single large enterprise or between different enterprises, provides significant opportunities for cost-effective access to large computational resources, promising to significantly enhance the scope and value of numerical simulation [1, 2]. For example, large-scale parallel high performance computing (HPC) applications may be tackled, or large parameter spaces explored through the use of multiple solutions of smaller problems. In this paper we present a new problem solving environment (PSE) that enables users to launch, and interact with, jobs that execute on remote Grid resources. As is typical, e.g. [3–5], the PSE has been implemented for one highly challenging engineering application, however the design allows other applications to be swapped in without the need for fundamental changes.

Features of the Grid-enabled environment include the ability to launch jobs onto one or more remote Grid resources, to obtain real-time intermediate results and visualise them locally, and to steer the remote simulation by altering parameters such as physical conditions, numerical parameters or even the underlying mathematical model. Furthermore the PSE allows remote collaborators, working from other sites, to join a simulation and to interact with it through both visualisation and steering.

This work builds on an earlier PSE [6–8] by adding flexible Grid-enabled functionality and through the use of a challenging engineering optimisation problem as an industrially motivated application.

The particular application that has been selected for this work comes from elastohydrodynamic lubrication (EHL) [9, 10]. This is described in detail in the following section. Section 3 then explains how the fundamental EHL problems are embedded within an optimisation procedure that is used for selecting the best possible parameter values within the simulation model.

Section 4 describes the necessary changes to turn the serial optimisation algorithm into a distributed memory parallel application with fast solution times. Consideration of the appropriate degree of parallelism for this application is given here. In Section 5 this work is extended to also include parallel solution for the numerical problem at the heart

of the optimisation process itself, hence achieving a hierarchy of parallelism: this is explained in the context of using distributed, remote Grid resources.

Having provided an explanation of the engineering application, and how it may be executed in parallel across a computational Grid, Section 6 focuses on the PSE itself. This is a vital tool in effective use of Grid resources since the ability to interact with a simulation, to guide the solution or to change the problem being solved, is very important. From a PSE this can be done without recompilation of code or resubmission of the job onto the Grid. As Grid cycle accountancy, through utility computing on demand, develops in the coming years it will be important not to have wasted clock cycles, and steering will assist with this. The Grid-enabling aspects of the PSE are also described in this section, along with a description of how the gViz collaborative libraries [11] are used. The output visualisations for such a complex problem are also very important in being able to effectively use the PSE and these are described in Section 6.3.

2 Elastohydrodynamic Lubrication Modelling

Elastohydrodynamic lubrication problems occur, for example, in lubricated journal bearings and gears where, at the centre of the contact region the load exerted over a very small area causes extremely high pressures (up to 3 G Pa) resulting in both elastic deformation of the components and significant changes in the lubricant properties in this area [9]. The mathematical models of these problems are therefore highly non-linear and provide challenging tests for reliable numerical simulation. In recent years there have been significant advances in the development of robust numerical methods for these problems, summarised by Venner and Lubrecht [10]. In this work we consider both one dimensional *line contact* cases, such as long (modelled by infinite) rollers, and two dimensional *point contact* cases, such as journal bearings.

Mathematically EHL is described by a highly non-linear integro-differential equation system relating the pressure, P, the geometry, H, the density, $\overline{\rho}$, viscosity, $\overline{\eta}$, and

temperature, θ, solutions. The steady-state governing equations are given, in non-dimensional form, by the following equations. First, the Reynolds Equation, shown here for the point contact, governs the pressure distribution for a given geometry:

$$\frac{\partial}{\partial X}\left(\varepsilon\frac{\partial P}{\partial X}\right)+\frac{\partial}{\partial Y}\left(\varepsilon\frac{\partial P}{\partial Y}\right)-\lambda\frac{\partial(\overline{\rho}H)}{\partial X} \quad =0, \tag{1}$$

where ε and λ are given by

$$\varepsilon=\frac{\overline{\rho}H^3}{\overline{\eta}\lambda(u_a+u_b)}, \tag{2}$$

and

$$\lambda=\frac{6\eta_0 R_x^2}{a^3 p_h}. \tag{3}$$

The film thickness equation defines the contact shape, for a given undeformed geometry $\mathscr{G}$. For line contact cases it is given by

$$H(X) \quad = \quad H_{00}+\mathscr{G}(X)-\frac{1}{\pi}\int_{-\infty}^{\infty}\ln\left|X-X'\right|P(X')\mathrm{d}X', \tag{4}$$

and for point contact cases by:

$$H(X,Y)=H_{00}+\mathscr{G}(X,Y)+\frac{2}{\pi^2}\int_{-\infty}^{\infty}\int_{-\infty}^{\infty}\frac{P(X',Y')\,\mathrm{d}X'\mathrm{d}Y'}{\sqrt{(X-X')^2+(Y-Y')^2}}, \tag{5}$$

where H_{00} is the central offset film thickness, which defines the relative positions of the surfaces if no deformation was to occur. The force balance equation,

$$\text{line contact:} \qquad \int_{-\infty}^{\infty}P(X)\,\mathrm{d}X=\frac{\pi}{2}, \tag{6}$$

$$\text{point contact:} \qquad \int_{-\infty}^{\infty}\int_{-\infty}^{\infty}P(X,Y)\,\mathrm{d}X\mathrm{d}Y=\frac{3\pi}{2}, \tag{7}$$

is also solved to provide conservation of applied force.

More complex models may also be used, such as thermal cases where the temperature is variable both within the lubricant and on the surfaces. A typical form of this model is described in [12]. The lubricant models used in this work are thermal versions of the Dowson and Higginson density expression [13] and the Roelands viscosity model [14]. Once solutions for these equations are found it is possible to derive the shear stress on each surface [12]. For example on surface 1 the force is defined to be

$$\overline{\tau}_{xz;1}(x) = -\frac{ap_hH}{2R}\frac{\partial P}{\partial X} + \frac{R}{a^2\eta_0}\frac{\overline{\eta}}{H}(U_2 - U_1) \tag{8}$$

$$\tag{9}$$

for surfaces 1 and 2 at $z = 0$ and $z = H$ respectively, moving at dimensionless speeds U_1 and U_2 respectively. From these expressions it is possible to work out the total friction through a contact. In the line contact case, for example, this is given by $\mathscr{F}$ as:

$$\mathscr{F} = \int_{-\infty}^{\infty} p_h \overline{\tau}_{xz;1}(x)\mathrm{d}x. \tag{10}$$

Example line contact solutions are shown in Figure 1 for (a) the pressure and surface geometry (film thickness), and (b) the density and effective viscosity. Note the existence of the pressure spike towards the outflow at the end of the contact region. This is a well known physical feature of these highly loaded EHL contacts, and clearly requires fine-scale numerical resolution.

In this work we make use of existing EHL software, described in [15–17]. More general information about the techniques used in numerically solving EHL problems may also be found in the work of Venner and Lubrecht [10]. Described briefly, the equations are discretised on a regular mesh of N=(2^k+1) points in each dimension. Both first and second order finite differences may be used. The resulting non-linear algebraic systems are solved using the multigrid techniques described in [10, 15, 16, 18] and the multi-level multi-integration (MLMI) algorithm of Brandt and Lubrecht [19]. MLMI uses coarse grids and high order grid transfer operations to reduce the deformation calcula-

tion (i.e. the integral in (5) from $\mathscr{O}(N^4)$ to $\mathscr{O}(N^2 \ln N^2)$. The single grid cost is so high since the discrete version of Equation (5) is a multi-summation of the entire fine domain, for each point. In this work we have used sixth order coarsening to restrict the finer grid solutions through a hierarchy of grids to the coarsest grid. It is on this coarsest grid that the multi-summation is performed, at a fraction of the cost. The calculated contributions to the deformation are then prolonged back through the hierarchy, correcting the approximation to the summation near each point by having a more accurate summation in the locale.

3 Optimisation for EHL

The EHL models described in the previous section contain a large number of parameters. These can be split into those describing the physical conditions of a particular test, and those describing the rheological properties of the lubricant being used. The physical parameters include the loading of the contact, the ambient temperature and *slide to roll ratio*, a measure of the amount of slip of one component past the other given by

$$\mathscr{S} = \frac{2(u_2 - u_1)}{u_1 + u_2}, \tag{11}$$

where u_1 and u_2 are the speeds of surfaces 1 and 2 respectively. The lubricant requires up to 40 parameters to specify its behaviour in a full non-Newtonian thermal EHL simulation. These parameters are not easily measured for a given lubricant and so a practical approach to assigning their values is to optimise these parameter values against measured experimental data for that lubricant.

The optimisation undertaken in this work is intended to find the set of lubricant model parameters that best match the total friction through the contact from numerical calculations to the observed friction in experiments performed on a test rig under a sequence of different physical conditions. In these examples the experiments have been run at three different loadings, two different ambient temperatures and six different slide to

roll ratios, giving a total of 36 different cases, covering a wide range of the operating conditions which lubricants may undergo in practice. By using a numerical solver it is possible to run each of these cases for a particular input parameter set. Ten of the lubricant rheology parameters have been varied to try to find the parameter set that most closely matches the frictional behaviour of the real lubricant. For a given set of lubricant parameters we define the total frictional residual, $\mathscr{R}_F$ to be

$$\mathscr{R}_F = \sum_{j=1}^{36} \left(\mathscr{F}_j^{num} - \mathscr{F}_j^{exp} \right)^2 \tag{12}$$

where $\mathscr{F}_j^{num}$ and $\mathscr{F}_j^{exp}$ are the numerical and experimental values of the friction for the j^{th} set of physical parameters, with the numerical value being calculated as given by Equation (10), or its two-dimensional generalisation for the point contact case. With ten physical parameters to vary the optimiser is thus trying to minimise $\mathscr{R}_F$ in ten dimensional space. Furthermore each evaluation of $\mathscr{R}_F$ requires 36 separate, computationally intensive, EHL problems to be solved.

The precise choice of optimisation algorithm used is not the focus for this work which is on the fast and efficient evaluation of the optimisation function (and possibly its derivatives) rather than the use of a particular minimisation code. For the examples given in this paper a sequential simplex algorithm [20, 21] has been used from the NAG C library [22]. This has the advantages of being simple, robust, and not requiring any derivatives to be found. Although not used here, gradient based algorithms could equally well have been employed, with gradients based upon finite difference or adjoint calculations, for example [23, 24]. For this work the choice of optimisation method is not important since the PSE is independent of the particular choice of minimisation algorithm.

Each evaluation of $\mathscr{R}_F$ incurs the cost of performing 36 EHL solutions, and the typical number of $\mathscr{R}_F$ evaluations required in a standard run is of the order of 10^3. An overall schematic of the optimiser is shown in Figure 2. This shows the dataflow with the

36 EHL cases at the bottom and different $\underline{x}_i$, lubricant parameter sets, being supplied by the optimiser from potential points in the simplex. Each EHL case returns an $\mathscr{F}_j$ contribution to the $\mathscr{R}_F$ value for this particular $\underline{x}_i$. Finally the optimiser returns a local minimum solution, $\underline{x}_{min}$, from the search space.

4 Parallelism of the Optimiser

In this section we focus on the EHL line contact problem. This is one-dimensional and hence each of the individual EHL problems fits easily into memory and may be solved efficiently on a single processor. This means that the first level of parallelism may be focused at the level of the optimiser which performs multiple EHL calculations for each $\mathscr{R}_F$ evaluation. Each of the calculations has identical lubricant characteristics but different operating conditions meaning that it is possible to run all the cases independently of each other, since the result of one does not influence any of the others. However there are great time savings to be made for EHL problems by using continuation methods. That is, the result to one problem is often a very good guess for the solution to a similar problem, hence by forming a chain of similar problems the relatively expensive 'first link' in the chain can then give the next result with far less computational effort.

The overall work per processor is sketched in Figure 3, where each processor performs one set of continued runs on a subset of the 36 EHL cases. The only communication necessary is the addition of each individual processor's contribution $\mathscr{R}_F^p$ to the global $\mathscr{R}_F$. Once the combined total has been accrued in parallel the optimiser itself continues to function as for the serial case.

The use of continuation adds an extra level of robustness to the solver. Table 1 compares various different continuation schemes and shows the results comparing the maximum number of processors (36) where no continuation is possible; continuation with increasing temperature (2 runs per processor); continuation with increasing loading (3 runs per processor); and continuation with increasing slide to roll ratio (6 runs per processor). It

can be clearly seen that maximising the amount of continuation used is very important for increasing the overall efficiency. Where more processors are used continuation between results is less frequent meaning more full restarts, and hence the parallel speed-up diminishes. The final line shows the comparative serial code using continuation along lines of increasing slide-to-roll ratio. The variation in the number of $\mathscr{R}_F$ evaluations to reach a local minimum is again due to the lack of continuation since a poor initial guess can cause the numerical solver not to converge, meaning that the calculated friction is given a 100% error for that case, therefore affecting the future behaviour of the simplex algorithm.

The parallel software from this project is designed for computational grids such as the White Rose Grid [25] with its mixture of shared and distributed memory machines, including a 256-processor Beowulf style cluster. For reasons of portability the parallelism is undertaken using MPI [26].

5 Parallelism of the Solver

The line contact problem discussed in the previous section illustrates how the optimisation process may be parallelised to increase the solution speed. The same optimisation process may also be used for 2-d point contact problems however the computational cost increases still further in this situation. This is overcome through the use of a parallel point contact solver, adapted from previous work [7, 27], in order to reduce the computational time sufficiently to make the optimisation feasible.

5.1 A parallel EHL point contact code

The starting point for the parallelisation of the method described above is the large amount of work done on parallel multigrid methods [28–31] and work by the authors on shared memory machines [7]. Discussions as to why parallelisation of multigrid, an already optimal algorithm, does not readily produce high parallel efficiencies are given by

McBryan *et al.* [30], Llorente *et al.* [28, 29] and Tuminaro and Womble [31]. The main problems are the frequency with which coarse grids are encountered, meaning that there are very high communications costs relative to the computation. This is especially true once the *critical level* has been reached, namely the coarse grid where each processor has the smallest non-trivial amount of computation. The choice left is whether to use the critical level as the coarsest in the multilevel scheme; to agglomerate, by moving all the work to a single processor as in Linden *et al.* [32, 33]; or to have idle processors, such as used by Brown *et al.* [34].

In the case of EHL problems the addition of MLMI causes extra difficulties as even more work is done at coarse mesh levels. In particular, since no significant computation is done during the MLMI coarsening the communication costs are already a large factor in terms of efficiency. A schematic of the overall algorithm is sketched in Figure 4 which shows a multigrid V cycle with multiple MLMI calls at each level. In contrast to the multigrid method the most striking change is that there is no calculation other than at the multi-summation and correction stages, all the work is in grid transfer.

The convergence properties of the standard solution methods mean that line solves are the most efficient multigrid smoothers for these problems [18, 35], and hence such smoothers have been considered during the parallelisation of the solver. The natural geometric domain decomposition is therefore that of strips in the direction of the lubricant entrainment. Due to regular grids being used in the solver, it is possible to ensure that coarser grids are always decomposed onto the same processors as their coincident finer grid points. This aids communication efficiency during grid transfer. More detailed discussion of grid transfer is given in [27].

The overall performance of the parallel solver is shown in Figure 5, where the timings are shown for a typical case on a grid of 4097×4097 points, on up to 64 processors. Note that as the number of processors increases the size of the coarsest grid increases too, in order to ensure that the coarsest grid can be partitioned across the processors. This leads to a loss of efficiency since the deformation calculation (using the MLMI algorithm) is

being done more accurately but at a much a higher overall cost. Conversely, if we fix the size of the coarsest mesh there is a maximum number of processors that may be used on it. For the cases shown in Figure 5, which is typical in this work, it is clear that there is little point in going beyond 16 processors on an individual EHL case. A more comprehensive discussion of these coarse grid issues may be found in [27], and ways of improving the situation are proposed, although these all add significantly to the complexity of the implementation.

In this work, however, it is clear from the previous section that additional parallelism is possible if we make use of a hierarchical approach which combines this parallel solver with the parallel optimisation described in the previous section. This aims to make optimal use of the Grid resources available, as outlined in Section 5.2 below, rather than simply using all the available processors on each single EHL case, which Figure 5 illustrates would be less efficient.

5.2 Hierarchical parallelism

The use of the parallel solver inside the parallel optimiser leads to the notion of *hierarchical parallelism*. This is illustrated in Figure 6 where the *Grid Master* can be seen to be communicating with a series *Simulation Controllers*, which, rather than being the EHL simulations as in the line contact work, are now the lead processes of parallel EHL simulations.

For reasons of portability the software produced in this work makes use of the MPI library [26]. In implementing this hierarchical strategy it has been necessary to introduce additional MPI communication groups, to include local groups for each simulation and a group for all of the Simulation Controllers. This latter group of processes is responsible for synchronisation at the end of each $\mathscr{R}_F$ evaluation, with each Simulation Controller posting its contribution to $\mathscr{R}_F$ to the Grid Master. The Grid Master then broadcasts within this group the necessary information (i.e. the parameter set $\underline{x}_i$) for the next $\mathscr{R}_F$ evaluation. Each Simulation Controller then passes the relevant information down to its

worker processes via the local simulation group.

This communication paradigm means that it is possible to take advantage of the Grid, rather than just traditional HPC technologies. In particular if, rather than a massively parallel machine, multiple smaller resources are available, then it is possible to use Globus with Grid-enabled MPI, MPICH-G2 [36], to split the computation sensibly between resources. This would allow frequent, data-heavy, high speed communication within single resources for each EHL simulation, but slower speed TCP/IP traffic between Grid resources transferring small amounts of data only at the end of each continuation series.

The solution speed for the hierarchical parallelism scheme is illustrated in Figure 7. This shows the time taken for ten $\mathscr{R}_F$ evaluations using the hierarchically parallel optimisation solver, each EHL solve consisting of ten multigrid V-cycles on a mesh of 1025×1025 points. It may be seen from this figure that the parallelisation of the optimiser, with parallelisation of the solver beneath is a good strategy. The issues concerned with the loss in efficiency beyond 48 processors are three fold. First, the grid resolution, and hence high level of coarse grid communication is starting to effect the parallel solution efficiency. The second issue is concerned with the EHL cases not all having the same computational solution time when the physical parameters are varied. Most importantly in a Grid setting, however, not all of the 96 processors used in this example are identical. Hence if one set of parallel computations takes place on a slower set of processors than the rest this will lead to a loss of overall efficiency. This last observation raises some interesting issues regarding dynamic load balancing across Grid resources, however these are beyond the scope of this paper.

6 A Grid-enabled PSE

Problem Solving Environments are a very useful way in which to combine simulation and visualisation into a single package. The consequential benefit of such a system

is that it facilitates experimentation with minimal additional effort from the user. It is the combination of these elements, combined with the knowledge of the user, that make such systems potentially very powerful for obtaining understanding of the range of problems being solved.

PSEs were first proposed by the landmark NSF report of Haber and McNabb [37] and have become more readily built as software systems, especially visualisation packages, have evolved. Commercial visualisation packages, such as NAG's IRIS Explorer [38], AVS, and IBM's OpenDX, all have functionality for including simulation components. Some open source PSEs have also been developed, most notable among them being SCIRun [39] which has grown out of a more focused PSE for a particular (medical) application, to become the more general system of its latest releases.

The integration of Grid technology with PSEs is now a natural step in this evolution. The ideas of 'workflow' in Grid terminology correspond very closely with how PSEs are generally constructed within any of the environments cited above. Besides the PSEs designed for EHL problems, which are clearly the most relevant to this paper, [6, 7], there are several other related works of note. A good example of a specific PSE being extended to massively parallel computers is Uintah [40] which has extended SCIRun through a common component architecture. Uintah is currently being developed further using the Globus toolkit, as is the Cactus project [41].

6.1 The gViz libraries

Much of the new Grid-enabling work described in this paper makes use of the gViz libraries which are described in full in [11]. In brief, gViz provides a communication interface for a process running on a (typically) Grid resource to enable other users to connect to the simulation and either visualise the results or steer the calculation. It does this by providing a library of functions for communication of data between separate programs.

A schematic for the gViz communications patterns is provided in Figure 8, which shows

the main desktop PSE being connected to a remote simulation through channels labelled ‘Grid’, ‘Visualise’ and ‘Steer’. The functions are described in detail in the following paragraphs. In addition Figure 8 also illustrates a second PSE that is able to connect with the remote simulation. A connection is indicated between the two PSEs themselves, representing the fact that some information may be shared at the desktop level, without involving the remote simulation. Examples of such include camera position, adding pointers to solution features, or sharing visualisation quantities.

When the simulation is launched from the main PSE it is important for the PSE to know where to find the simulation, so that it can initiate the necessary connections through the use of sockets. In the simplest scenario the ‘launcher’ specifies as command line arguments its machine name and a specific port on which it will be listening. The simulation then uses this advertised location to return the location of the running threads. This destination location is kept the same for all new listeners to connect through. This is referred to in Figure 8 as the ‘Grid’ channel. A more complicated scenario involves the use of a gViz directory service. If specified at launch time then the simulation will register here rather than with the desktop PSE. This enables the location of the running simulation to be advertised in a more persistent manner, thereby aiding other desktop PSEs wishing to connect for the purposes of collaboration or asynchronous steering.

Once the simulation on the Grid resource is running it must start its own ‘Visualise’ and ‘Steer’ channels. This is done through separate threads which wait until a “listener” makes a connection. If a connection is made to one of these threads then an additional thread will start and wait for the next listener. When the connection to a listener is terminated, the thread is also closed to free the memory and the port. Throughout the execution of the simulation it is these ‘Steer’ and ‘Visualise’ channels along which data flows. User requests for computational steering are sent via the ‘Steer’ channel. The main simulation thread will query the steering thread at suitable intervals to receive any updates. The steering data is a predefined list of inputs to the simulation and hence this is usually a relatively short list. Through the gViz functions a user may change one or

multiple values at any time. Steering information is synchronised between connected PSEs so changes made by one user are reflected on the desktop of any others.

Whenever an output dataset is ready it is made available through the 'Visualise' channel. This data is typically far larger in quantity, and less regularly defined, than the steering data and hence gViz requires the application developer to make available all the information needed by the desktop PSEs to create a visualisation. Typically this data is broken down into coherent blocks of similar data, such as coordinates of mesh points, and solutions values, along with basic variables such as the number of dimensions and the number of datasets being returned. In order to receive this information the desktop PSE must allocate memory of the appropriate size and so after receiving the number of blocks being sent, the simulation will transmit the number of bytes in each block. The PSE-end of the application can then convert the raw data into native data formats for the particular PSE being used. Any listeners connecting to the simulation are able to receive the latest dataset and hence all such information is retained at the simulation end, rather than on the desktop. Visualisation conversions from gViz to PSE-package specific formats have been successfully implemented for IRIS Explorer, SCIRun, Matlab and VTK. Note that since raw data is being returned through the 'Visualise' channel, different PSEs may choose to perform very different visualisations at the same time.

6.2 Architecture

An example of a typical IRIS Explorer map for the EHL lubricant parameter optimisation PSE is shown in Figure 9 where the dataflow pipeline, generally from left to right, is clearly visible. The majority of the modules are used in the visualisation process and hence only the three modules on the left are described in the following paragraphs.

The first module in the map shown in Figure 9, *GlobusSearch*, interrogates a GIIS (Grid Index Information Service) server to analyse the available resources and their current statuses [42]. The user can then select a resource and choose a suitable launch method, including launching the job onto the Grid using Globus [43]. For this work we have ex-

tended the gViz library to include parallel launch mechanisms including writing a parallel job submission script or a Globus RSL (Resource Specification Language) script which then gets submitted to Sun Grid Engine for scheduling onto a suitable node. When the job is launched only one of the parallel processes will initiate the gViz library and handle the communication between the Grid job and the desktop PSE. The information returned to the desktop, described above, detailing the location of the Grid job is then passed to the next two modules in the map, *SteerGOSPEL* and *VisualiseGOSPEL*. Knowledge of where the simulation is running also allows any other user to access the simulation through the gViz libraries. This means that one person, with Grid certification, can start the simulation and other collaborators around the world can then all see the results of that simulation and help to steer the computation [8,42]. In fact, the person who originally launched the Grid job need not actually be involved from that point on.

Computational steering is the ability to change a simulation that is already running. One example of this could be choosing to use a lower quality mesh in the early stages of the solve, but as the solution gets near to a local optimum using a higher resolution mesh to improve the accuracy of the solution obtained. The module *SteerGOSPEL* has several uses. Firstly it shows the current best set of values found by the optimisation algorithm, along with $\mathscr{R}_F$. This allows a user access to individual numbers from the simulation rather than much larger datasets for visualisation purposes. These numbers can also be used for steering. For example it is possible to resubmit this current best set to the optimiser once a minimum has been found. The simplex algorithm will then build a new simplex around this previous minimum, potentially allowing it to escape from local minima. Similarly, a different point in the search space can be specified away from regions in which the optimiser has previously searched. Alternatively, as mentioned above, the accuracy can be changed. A further method that we have implemented in this work is the ability to change the underlying mathematical model being used. In the case of EHL simulations, for example, we permit the user to turn on (or off) the thermal components of the solution. The thermal solve (i.e. treating temperature as a variable

across the contact through addition of an energy equation) is much more expensive but adds greater accuracy to the friction results obtained, especially for those cases where more heat is generated [15].

Communication from the PSE to the simulation is done, as described above, through the gViz libraries. At suitable points the simulation will check if any new input data has been received. If a steering request is for additional accuracy, say, then these changes can be introduced without changing the points of the current simplex and would therefore only apply to future calculations. If, on the other hand, a new simplex was requested then the use of a communication flag inside the routine will cause the optimisation routine to terminate and then restart with the new simplex.

The *VisualiseGOSPEL* module communicates with the simulation to receive all of the datasets for visualisation. These are then packaged up into standard IRIS Explorer datatypes and sent down the rest of the map for visualisation. When the full datasets are being shown then more information needs to be returned from the parallel nodes than is necessary for just the optimisation process. Descriptions of the most significant output datasets are provided in the following section.

6.3 Visualisation

A full optimisation run generates very large quantities of high-dimensional multivariate data even though each single EHL simulation is reduced to just one number, $\mathscr{F}_j^{num}$, from Equation (12). The distance each of these calculated values is away from $\mathscr{F}_j^{exp}$ is one piece of information that may be of interest to a user wishing to steer the optimisation. For example if the results were all good except at, say, very high ambient temperatures then engineering knowledge of which parameters affect the accuracy at such temperatures could be used to accelerate the optimisation process. A visualisation of such data is shown in Figure 10 which consists of a 2-d plane with increasing slide to roll ratios plotted against experimental friction for each of the loadings and ambient temperatures. The 3-d surface represents the errors in each of the calculated friction

values. If a perfect solution was found this would collapse to lie exactly on the six lines of experimental results.

The progress of the optimiser itself may also be visualised. The most useful information would be to display the evolution of the best data set found thus far, however this high-dimensional data cannot be represented easily. Other techniques are therefore required to allow the user to visualise the progress of the optimiser. One of these is shown in Figure 11 where the *y*-axis represents the relative change from the initial estimate for each of the ten variable parameters, with progression along the *x*-axis being the incremented for improvements in the $\mathscr{R}_F$ value. In Figure 11 two different graphs are shown. The first has the optimiser progressing without any steering, whilst the second has a new simplex formed after the 80^{th} improvement to the best point in the simplex, see Figure 12. It is clear from Figure 12 that the new converged value is better than the pre-steered converged value. Combining this information with the change in converged solutions as shown in Figure 11 we can see that this significant improvement has been obtained even though most of the individual parameters are similar to those reached for the previous (local minimum) solution.

Other visualisation techniques are possible and have been implemented. The choice of the most appropriate visualisation techniques to use is clearly dependent on the particular simulation being performed. Another approach that we have implemented is based upon the use of parallel coordinates [44], where each component of the solution is visualised as a vertical displacement on a 2-d graph. These can be useful for identifying dependencies between variables.

7 Evaluation

In this work we have demonstrated how a complex serial, engineering optimisation code may be efficiently parallelised, Grid-enabled and embedded within a PSE. Through the use of the PSE it is possible for an engineer user to experiment more easily by tak-

ing advantage of the benefits of concurrent simulation and visualisation, and the use of computational steering. The specific visualisation demands for this particular application are driven by the needs of the users, so as to help them to gain insight into a multidimensional parameter space; enabling them to escape from local minima, as well as understanding the nature of the EHL simulations being computed. The use of parallelism in the simulation has decreased the real-time execution of the simulation significantly and the hierarchical parallelism approach has facilitated tackling much more complex optimisation problems than had previously been feasible. The use of MPI for the parallelism has allowed portability between Grid resources, and use of the open source gViz libraries has ensured that the communication between different platforms of PSE and Grid resource is similarly transparent.

In order to transform the PSE demonstrated in this work to a different problem domain the following issues would need to be considered.

- Inputs – for many real engineering applications there can be large numbers of input quantities used in the software. These will be a mixture of physical descriptions, numerical parameters for the solver, and perhaps even choices of solution methods to be used. Deciding which of these to expose to the user will depend on their level of expertise.

- Steering – it is necessary to decide which of the input quantities to steer based upon how changes in each of these are likely to affect the progress of the solver. For instance in our scenario increasing the resolution of the domain is a relatively minor change compared with switching the oil being tested.

- Outputs – choice of precisely what data to make available for output visualisations can be non-trivial. In cases such as the optimisation example of this paper, the large numerical solutions to the individual cases will generally be reduced to just a few numbers, but these can be combined with other related results to produce more detailed understanding.

- Parallelism – we have demonstrated that the use of hierarchical parallelism can be highly beneficial. However we have also seen that whenever there are independent cases being solved results may be strung together in continuation chains to reduce the degree of parallelism, but increase the overall performance. This issue is therefore possibly the most problem specific matter that must be considered when transforming the PSE.

At least two significant generic conclusions may be drawn from this work. The concept of not only running a computationally intensive code on remote Grid resources, but also of interacting with it in real time, has been demonstrated to be feasible for a non-trivial engineering test-problem. This has important implications for the ways in which computational scientists and engineers may work with large-scale off-site compute resources, as well as allowing physically distributed team members to interact with Grid-based simulations. Furthermore the concept of hierarchical parallelism, in which a task is partitioned across more than one parallel computational resource on the Grid, has also been demonstrated to be a powerful practical tool for Grid computing. This particular research conclusion is of potential significance whenever an ensemble of computationally intensive calculations are required, not only for optimisation problems of the type considered here, but also when sensitivity analysis is necessary or when numerical derivatives are being calculated for example.

One of the main areas for future expansion of these ideas is to undertake additional research and development into the effective incorporation of data security. The data used in engineering simulations is often commercially sensitive and so secure methods of communicating this to and from remote Grid resources must be considered. This particular work was undertaken using the White Rose Grid [25] which has a number of standard security devices implemented, but is not designed to have the same levels of security that one would expect from within a single organisation.

Another area for future expansion concerns more general bookkeeping. When multiple simulations are running and a new user wants to join in a collaboration, they may need

to know more than the name and location of each simulation currently listed in the directory service. More detailed information such as steering histories and current active users could be very useful.

The final area of future research that we highlight here is that of dynamic load balancing on the Grid. As we have seen in this work, when a job is partitioned across more than one architecture on the Grid it is not necessarily a good load balancing strategy to assume that all processors have the same performance. It would be helpful to establish a robust dynamic load balancing strategy that could move work between resources as and when it identified imbalances in their utilisation.

Acknowledgements

The authors wish to thank the DTI and EPSRC for funding this work with Shell Global Solutions through Core Programme e-Science grant number GR/S19486/01. Jason Wood is also gratefully acknowledged for supplying and supporting the gViz library used in this work.

References

[1] G. C. Fox and W. Furmanski. High performance commodity computing. In I. Foster and C. Kesselman, editors, *The Grid 2: Blueprint for a New Computing Infrastructure*, pages 237–255. Morgan Kaufmann, 2004.

[2] K. L. Wang and A. J. Baker. A modular collaborative parallel CFD workbench. *Journal of Supercomputing*, 22(1):45–53, 2002.

[3] C. R. Johnson, M. Berzins, L. Zhukov, and R. Coffey. SCIRun: Application to atmospheric dispersion problems using unstructured meshes. In M. J. Baines, editor, *Numerical Methods for Fluid Mechanics VI*, pages 111–122. ICFD '98, Oxford, 1998.

[4] H. Wright, K. W. Brodlie, and T. David. Navigating high-dimensional spaces to support design steering. In *VIS 2000*, pages 291–296. IEEE, 2000.

[5] D. Dabdub, K. M. Chandy, and T. T. Hewett. Managing specificity and generality: tailoring general archetypal PSEs to specific users. In E. N. Houstis, J. R. Rice, E. Gallopoulos, and R. Bramley, editors, *Enabling Technologies for Computational Science: Frameworks, Middleware and Environments*, pages 65–77. Kluwer Academic Publishers, Boston / Dordrecht / London, 2000.

[6] C. E. Goodyer and M. Berzins. Eclipse and Ellipse: PSEs for EHL solutions using IRIS Explorer and SCIRun. In P. M. A. Sloot, C. J. K. Tan, J. J. Dongarra, and A. G. Hoekstra, editors, *Computational Science, ICCS 2002 Part I, Lecture Notes in Computer Science*, volume 2329, pages 521–530. Springer, 2002.

[7] C. E. Goodyer, J. Wood, and M. Berzins. A parallel Grid based PSE for EHL problems. In J. Fagerholm, J. Haataja, J. Järvinen, M. Lyly, P. Råback, and V. Savolainen, editors, *Applied Parallel Computing, Proceedings of PARA '02, Lecture Notes in Computer Science*, volume 2367, pages 523–532. Springer, 2002.

[8] M. A. Walkley, J. Wood, and K. W. Brodlie. A distributed collaborative problem solving environment. In P. M. A. Sloot, C. J. K. Tan, J. J. Dongarra, and A. G. Hoekstra, editors, *Computational Science, ICCS 2002 Part I, Lecture Notes in Computer Science*, volume 2329, pages 853–861. Springer, 2002.

[9] D. Dowson. Elastohydrodynamic and micro-elastohydrodynamic lubrication. *WEAR*, 190:125–138, 1995.

[10] C. H. Venner and A. A. Lubrecht. *Multilevel Methods in Lubrication*. Elsevier, 2000.

[11] J. W. Wood, K. W. Brodlie, and J. P. R. Walton. gViz: Visualization and computational steering for e-Science. In S. Cox, editor, *Proceedings of the All Hands Meeting 2003*, pages 164–171. EPSRC, 2003. ISBN: 1-904425-11-9.

[12] L. E. Scales. Quantifying the rheological basis of traction fluid performance. In *Proceedings of the SAE International Fuels and Lubricants Meeting, Toronto, Canada*. Society of Automotive Engineers, 1999.

[13] D. Dowson and G. R. Higginson. *Elasto-hydrodynamic Lubrication, The Fundamentals of Roller and Gear Lubrication*. Permagon Press, Oxford, Great Britain, 1966.

[14] C. J. A. Roelands. *Correlational Aspects of the viscosity-temperature-pressure relationship of lubricating oils*. PhD thesis, Technische Hogeschool Delft, The Netherlands, 1966.

[15] R. Fairlie, C. E. Goodyer, M. Berzins, and L. E. Scales. Numerical modelling of thermal effects in elastohydrodynamic lubrication solvers. In D. Dowson *et al.*, editor, *Trobological Research and Design for Engineering Systems, Proceedings of the 29th Leeds-Lyon Symposium on Tribology*, pages 675–683. Elsevier, 2003.

[16] C. E. Goodyer. *Adaptive Numerical Methods for Elastohydrodynamic Lubrication*. PhD thesis, University of Leeds, Leeds, England, 2001.

[17] C. E. Goodyer, R. Fairlie, D. E. Hart, M. Berzins, and L. E. Scales. Calculation of friction in steady-state and transient ehl simulations. In A.A. Lubrecht and G. Dalmaz, editors, *Transient Processes in Tribology: Proceedings of the 30th Leeds-Lyon Symposium on Tribology*. Elsevier, 2004.

[18] C. H. Venner. *Multilevel Solution of the EHL Line and Point Contact Problems*. PhD thesis, University of Twente, Endschende, The Netherlands, 1991. ISBN 90-9003974-0.

[19] A. Brandt and A. A. Lubrecht. Multilevel matrix multiplication and fast solution of integral equations. *Journal of Computational Physics*, 90(2):348–370, 1990.

[20] J. A. Nelder and R. Mead. A simplex method for function minimization. *Computing Journal*, 7:308–313, 1965.

[21] J. M. Parkinson and D. Hutchinson. An investigation into the efficiency of variants on the simplex method. In F. A. Lootsma, editor, *Numerical Methods for Nonlinear Optimization*, pages 115–135. Academic Press, 1972.

[22] NAG. C software library.

[23] A. Jameson, L. Martinelli, and N. A. Pierce. Optimum aerodynamics design using the Navier-Stokes equations. *Theoretical Computational Fluid Dynamics*, 10:213–237, 1998.

[24] M. B. Giles and N. A. Pierce. An introductiond to the adjoint approach to design. *Flow, Turbulence and Combustion*, 65:393–415, 2000.

[25] P. M. Dew, J. G. Schmidt, M. Thompson, and P. Morris. The White Rose Grid: practice and experience. In S. Cox, editor, *Proceedings of the All Hands Meeting 2003*, pages 172–179. EPSRC, 2003. ISBN: 1-904425-11-9.

[26] Message Passing Interface Forum. MPI: A message-passing interface standard. *International Journal of Supercomputer Applications*, 8(3/4), 1994.

[27] C. E. Goodyer and M. Berzins. Efficient parallelisation of a multilevel elastohydrodynamic lubrication solver. *Concurrency*, submitted.

[28] I. M. Llorente, M. Prieto-Matías, and B. Diskin. An efficient parallel multigrid solver for 3-d convection-dominated problems. Technical Report TR-2000-29, ICASE, 2000.

[29] M. Llorente, F. Tirado, and L. Vázquez. Some aspects about the scalability of scientific applications on parallel computers. *Parallel Computing*, 22:1169–1195, 1996.

[30] O. A. McBryan, P. O. Frederickson, J. Linden, A. Schuller, K. Solchenbach, K. Stuben, C.-A. Thole, and U. Trottenberg. Multigrid methods on parallel com-

puters – a survey of recent developments. *Impact of Computing in Science and Engineering*, 3:1–75, 1991.

[31] R. S. Tuminaro and D. E. Womble. Analysis of the multigrid FMV cycle on large-scale parallel machines. *SIAM Journal of Scientific Computation*, 14(5):1159–1173, 1993.

[32] J. Linden, G. Lonsdale, H. Ritzdorf, and A. Schüller. Block-structured multigrid for the navier-stokes equations: experiences and scalability questions. In *Visualization Development Environments 2000 Proceedings*, volume Proceedings of the Conference on Parallel Computational Fluid Dynamics 1992, Amsterdam, 1992. Elsevier Science Publishers B.V.

[33] J. Linden, G. Lonsdale, H. Ritzdorf, and A. Schüller. Scalability aspects of parallel multigrid. *Future Generation Computer Systems*, 10(4):429–449, 1994.

[34] P. N. Brown, R. D. Falgout, and J. E. Jones. Semicoarsening multigrid on distributed memory machines. *SIAM Journal on Scientific Computing*, 21(5):1823–1834, 2000.

[35] E. Nurgat, M. Berzins, and L. E. Scales. Solving EHL problems using iterative, multigrid and homotopy methods. *Trans. ASME, Journal of Tribology*, 121(1):28–34, 1999.

[36] N. Karonis, B. Toonen, and I. Foster. MPICH-G2: A Grid-enabled implementation of the Message Passing Interface. *Journal of Parallel and Distributed Computing*, 63(5):551–563, 2003.

[37] R. B. Haber and D. A. McNabb. Visualization idioms : A conceptual model for scientific visualization systems. In B. Shriver G.M. Nielson and L.J. Rosenblum, editors, *Visualization in Scientific Computing*, pages 74–93. IEEE, 1990.

[38] J. P. R. B. Walton. Now you see it – interactive visualisation of large datasets. In C. A. Brebbia and H. Power, editors, *Applications of Supercomputers in Engineering III*. Computatational Mechanics Publications / Elsevier Applied Science, 1993.

[39] C. Johnson, S. Parker, C. Hansen, G. Kindlmann, and Y. Livnat. Interactive simulation and visualization. *IEEE Computer*, 32(12):59–65, 1999.

[40] D. de St. Germain, J. McCorquodale, S. Parker, and C. R. Johnson. Uintah: A massively parallel problem solving environment. In *Ninth IEEE International Symposium on High Performance and Distributed Computing*, 2000.

[41] G. Allen, E. Seidel, and J. Shalf. Scientific computing on the grid. *Byte*, pages 24–32, Spring 2002.

[42] K. W. Brodlie, S. Mason, M. Thompson, M. A. Walkley, and J. W. Wood. Reacting to a crisis: benefits of collaborative visualization and computational steering in a Grid environment. In *Proceedings of the All Hands Meeting 2002*, 2002.

[43] I. Foster and C. Kesselman. Globus: A metacomputing infrastructure toolkit. *International Journal of Supercomputer Applications*, 11(2):115–128, 1997.

[44] A. Inselberg, T Chomut, and M. Reif. Convexity algorithms in parallel coordinates. *Journal of the ACM*, 34(4):765–801, 1987.

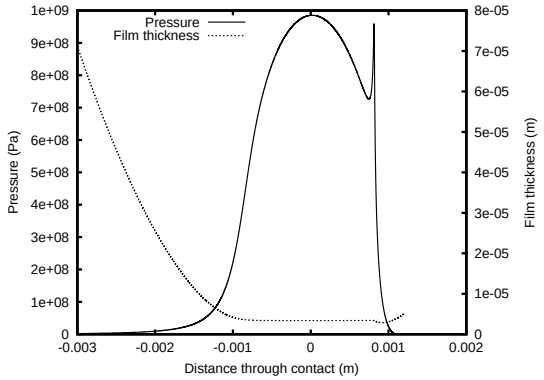

(a) Pressure (left hand axis) and film thickness

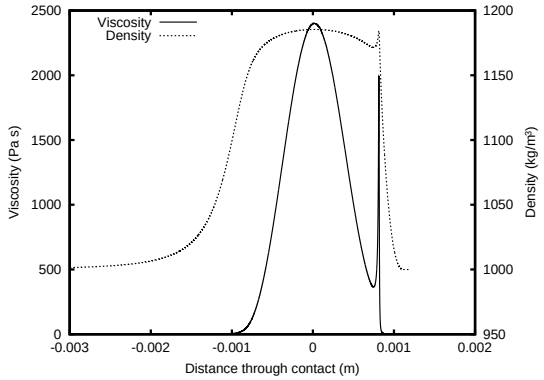

(b) Effective viscosity (Left hand axis) and density

Figure 1: Solution profiles of an EHL line contact

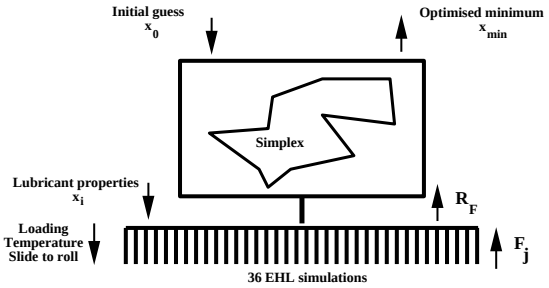

Figure 2: Optimiser schematic

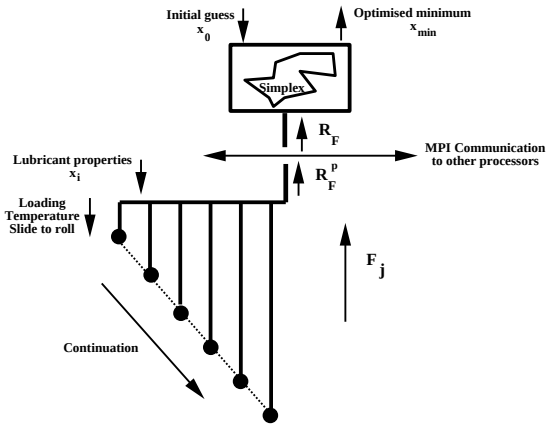

Figure 3: Parallel optimiser schematic

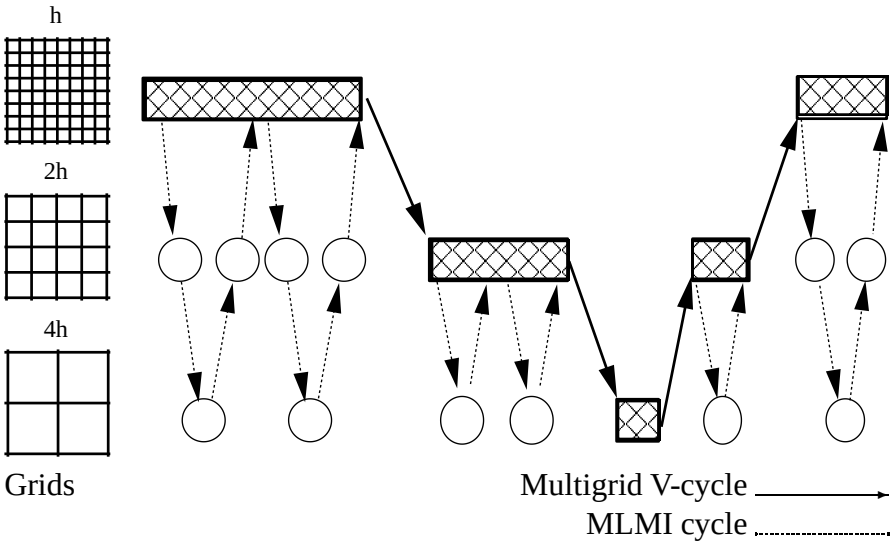

Figure 4: Example of a V cycle with MLMI at each stage

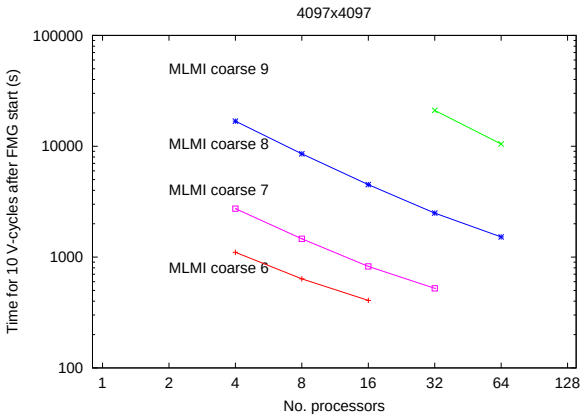

Figure 5: Parallel solution times for a 4097×4097 point case with differing levels of multilevel multi-integration

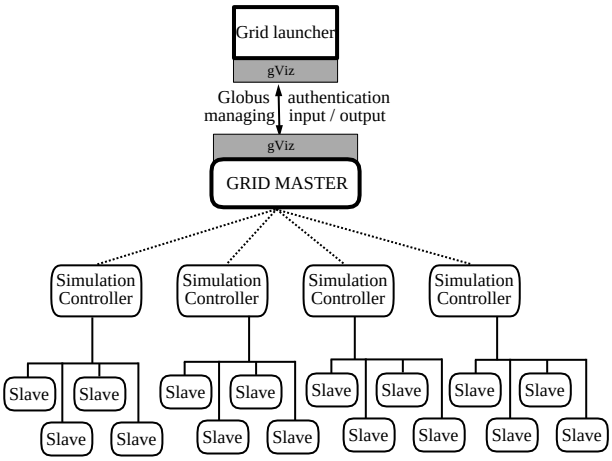

Figure 6: Schematic of the Grid-enabled optimisation solver using hierarchical parallelism

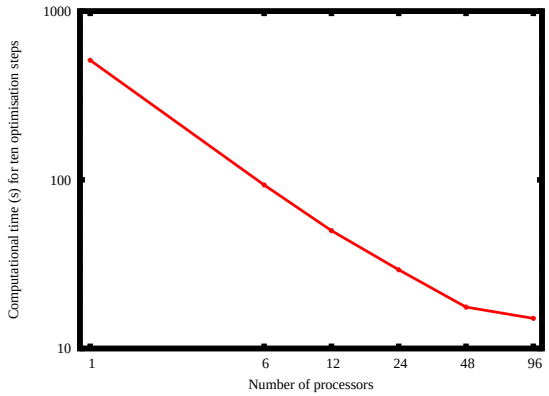

Figure 7: Computational time for hierarchically parallel optimisation solver

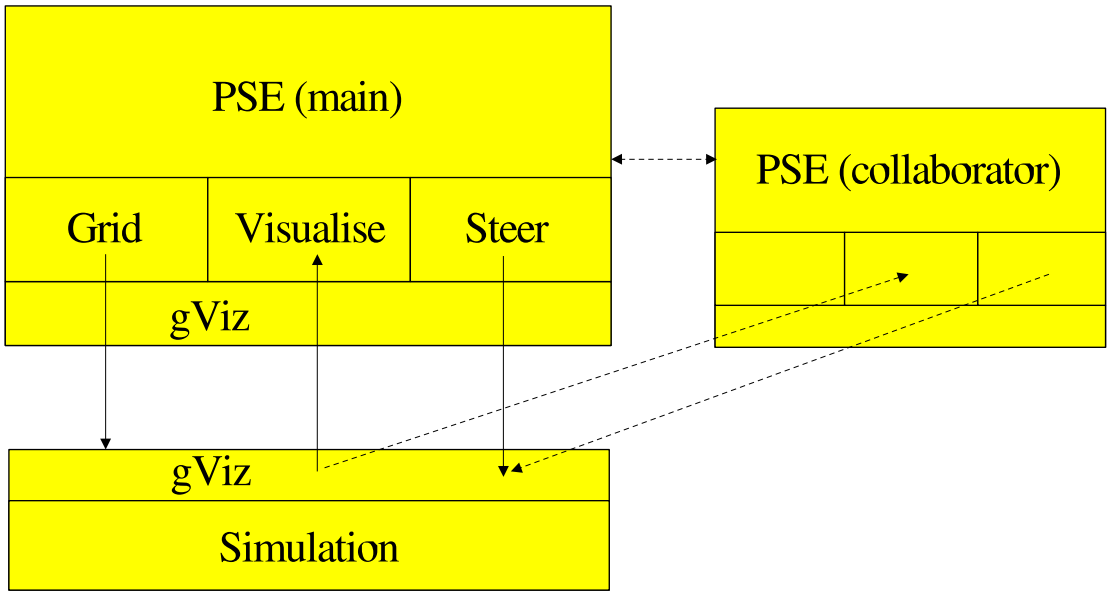

Figure 8: Schematic of how gViz provides the data transfer layer between the Grid and PSE processes

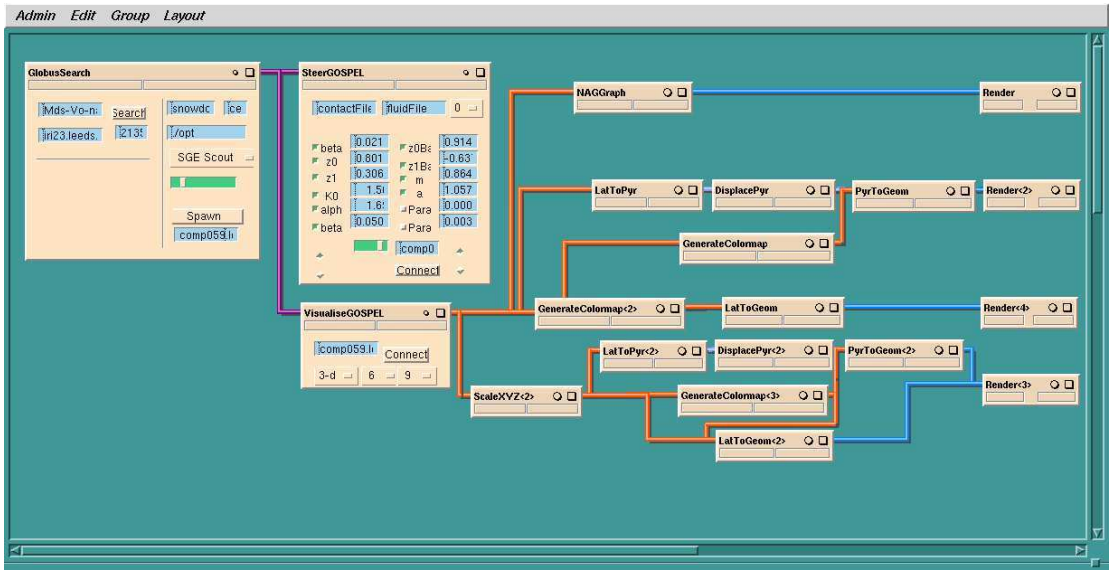

Figure 9: IRIS Explorer map of the PSE. Dataflow represented by wires between modules.

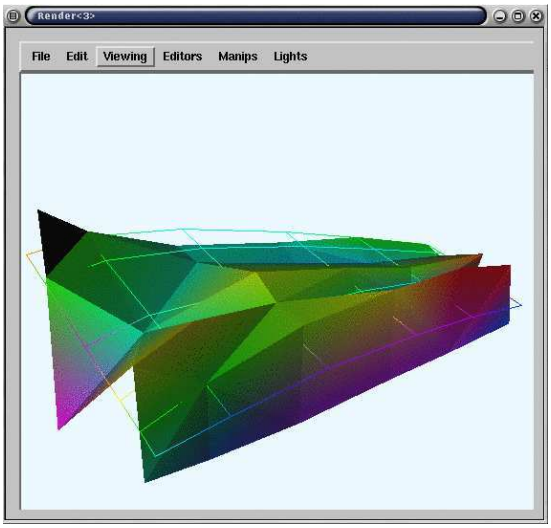

Figure 10: Friction errors for all cases considered. The 2-d mesh shows the experimental friction values against the slide-to-roll ratio with the displacement of the surface in the third dimension representing the error in the numerically calculated friction for the best simplex point.

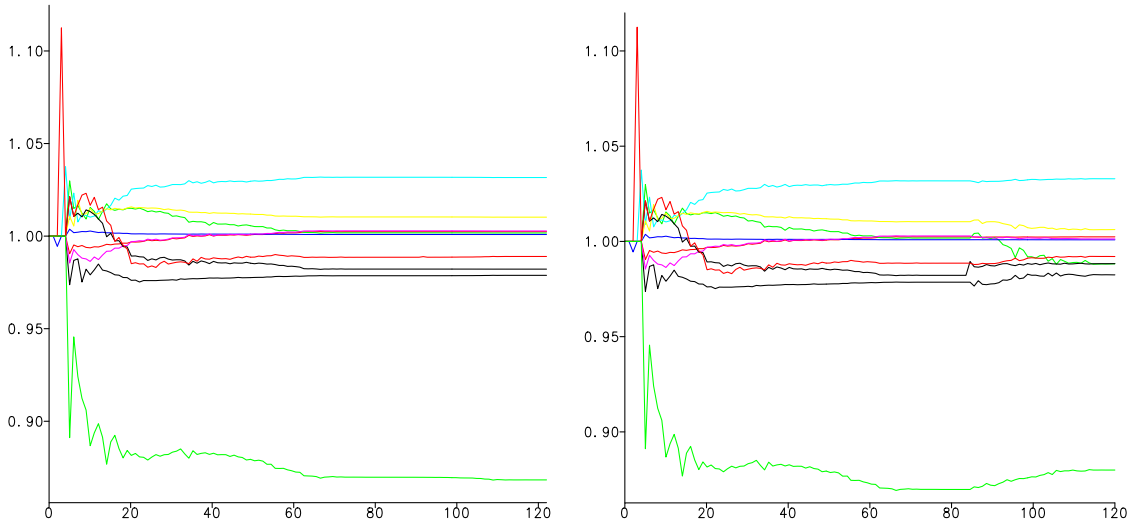

(a) No steering (b) New simplex after 80 improvements

Figure 11: Progression of optimiser showing relative change of best solution found to initial guess, with steering after 80 steps to escape a local minimum. Each line represents a different optimised parameter

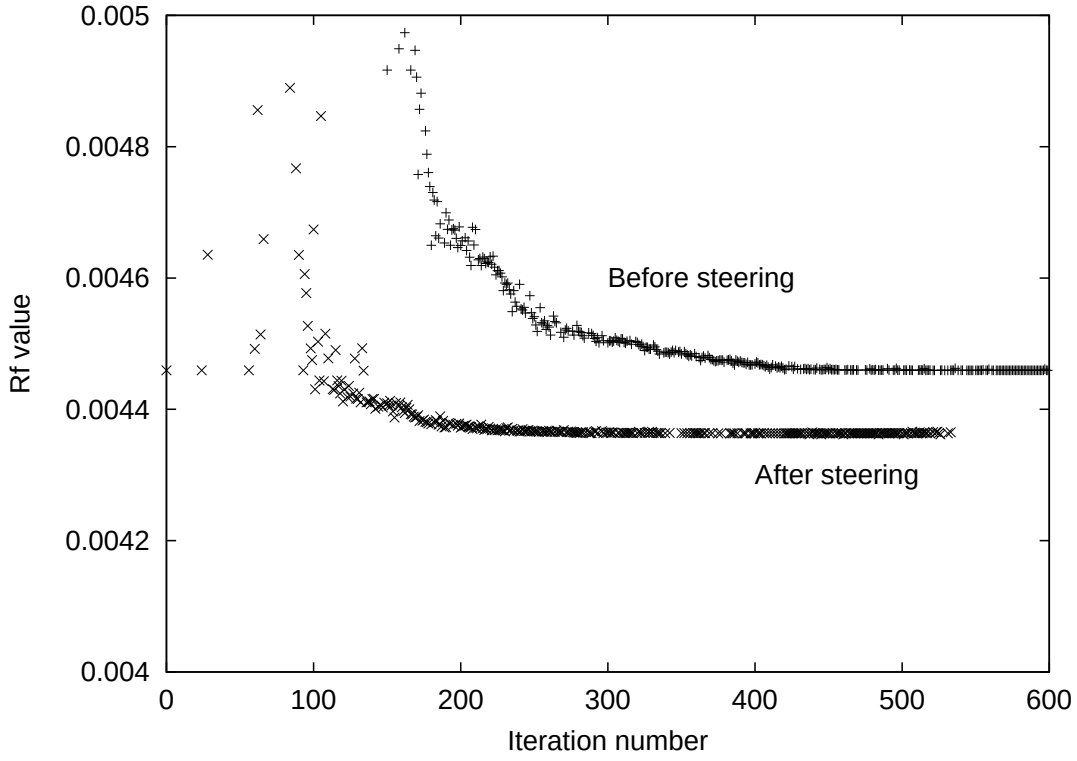

Figure 12: Convergence of the $\mathscr{R}_F$ value, before ($+$) and after ($\times$) steering; the iteration numbering starts from when the new simplex is formed

Continuation scheme	Processors	Solution time (s)	Number of $\mathscr{R}_F$ evaluations	Average time per $\mathscr{R}_F$ evaluation (s)
No continuation	36	2062	1009	2.04
Temperature	18	559	254	2.20
Loading	12	341	163	2.09
Slide to roll	6	531	217	2.45
Slide to roll	1	2560	217	11.80

Table 1: Optimiser solution times for varying continuation schemes